

Deactivation Pathways of an Isolated Green Fluorescent Protein Model Chromophore Studied by Electronic Action Spectroscopy

Matthew W. Forbes and Rebecca A. Jockusch*

Department of Chemistry, University of Toronto, Toronto, Ontario, Canada M5S 3H6

Received August 13, 2009; E-mail: rjockusc@chem.utoronto.ca

The green fluorescent protein (GFP) and its homologues are important tools for direct visualization of proteins in cells using fluorescence microscopy.^{1a} The barrel-shaped conformation of the folded protein provides a stabilizing environment for the light-emitting chromophore buried at its center.^{1b,c} Upon protein denaturation, the fluorescence is lost. How the protein fold enables fluorescence is not well-understood. The suggestion that the interior of the protein's barrel provides a gas-phase-like environment for the chromophore² led us to ask whether the chromophore, isolated in the gas phase, fluoresces significantly or whether other deactivation channels prevail.

Wild-type GFP has two characteristic absorption bands at room temperature, A (395–397 nm) and B (470–475 nm), ascribed to the neutral and anionic states of the chromophore, respectively.^{3a–c} Emission from the anionic state gives rise to the intense green fluorescence ($\lambda_{\text{max}}^{\text{em}} = 504 \text{ nm}$, $\Phi_f = 0.79$).^{3b,d}

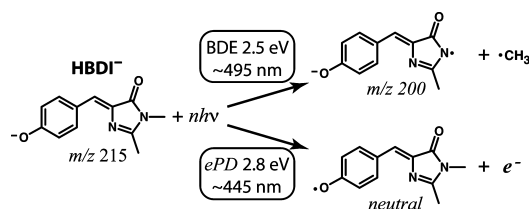
To better understand the intrinsic photophysical properties of the chromophore independently from the protein, numerous spectroscopic⁴ and computational studies⁵ have investigated synthetic analogues of the GFP chromophore (see the Supporting Information for additional references). The GFP model chromophore *p*-hydroxybenzylidene-2,3-dimethylimidazolone (HBDI, Scheme 1) exhibits an electronic absorption spectrum in solution that is significantly blue-shifted relative to that of the intact protein.^{4c} Ultrafast internal conversion of HBDI in room-temperature solutions effectively out-competes fluorescence as a deactivation pathway;^{4d,e} however, fluorescence activity is restored at 77 K.^{4b}

An important link between the properties of the chromophore buried inside the protein and those of the model chromophore has been provided by gas-phase investigations using photodestruction spectroscopy. Experiments on gaseous HBDI[−], photodissociated in the electrostatic heavy-ion storage ring at Aarhus (ELISA), detected a single, broad electronic absorption band ($\lambda_{\text{max}}^{\text{ab}} = 479 \text{ nm}$) that closely matches absorption band B of the native protein, suggesting that the protein scaffold provides an environment similar to the gas phase.²

We have constructed an apparatus to measure laser-induced fluorescence and photodissociation action spectra of mass-selected ions trapped in a modified quadrupole ion trap (QIT) mass spectrometer.⁶ Briefly, gas-phase ions are generated using electrospray ionization and stored in the QIT, where they are mass-selected and then irradiated with the frequency-doubled tunable output of a Ti:sapphire laser (80 MHz repetition rate, ~130 fs pulse duration). Fluorescence is collected orthogonally to the excitation beam and dispersed. Photodissociation action spectra are constructed by monitoring the disappearance of the precursor ion and appearance of product ions as a function of laser irradiation wavelength.

Irradiation of the isolated precursor ion HBDI[−] (*m/z* 215) with 470 nm light revealed no detectable fluorescence between 480 and 1100 nm (Figure S2 and Table S1 in the Supporting Information). Gaseous HBDI[−] does absorb 470 nm light, as shown by the ~20%

Scheme 1



photofragmentation yield observed upon irradiation. Dispersed fluorescence was readily observed ($S/N \approx 25$ at λ_{max}) from dyes such as gaseous rhodamine 575 under the same conditions (Figure S2). These results indicate that the isolated GFP chromophore has a low or negligible fluorescence quantum yield at room temperature in the gas phase, in line with the rapid internal conversion measured in the condensed phase.^{4d,e}

The dominant fragment ion observed upon photoactivation is at *m/z* 200, corresponding to the loss of a methyl group (Scheme 1). However, the intensity of the *m/z* 200 product ion was significantly less than the depletion of the precursor ion (Figure S3). In contrast, analogous experiments on protonated HBDI showed 98% recovery of ion yield (Figure S4). Evidently, an additional dissociation pathway is accessed by HBDI[−] in these experiments.

Electron photodetachment (*ePD*) from anions is a well-known mechanism of ion deactivation⁷ and is a probable explanation for the observed loss of ion signal (Scheme 1). The B3LYP/6-311+G(d,p)-computed bond dissociation energy (BDE) for the fragmentation channel (~2.5 eV) is similar to the computed adiabatic electron detachment energy (~2.8 eV). Both channels are in the range of the photon energies used here. For singly charged anions, neither product of electron detachment (the neutral species or the detached electron) is stored or detected in the QIT. Here, the extent of electron detachment was inferred from the difference between the precursor ion intensity *without* irradiation and the sum of the precursor and product ion intensities following irradiation (eq S4 in the Supporting Information).

To investigate the wavelength dependence of the *ePD*, we measured the photodissociation action spectrum of gaseous HBDI[−] in the QIT. Figure 1a shows the fractional depletion of HBDI[−] as a function of irradiation wavelength. The maximum at 482.5 nm is consistent with findings from ELISA,² yet the overall profile spans a much broader spectral range than that found in the storage ring experiments, with a strong feature present 1500 cm^{-1} above the band origin at 482.5 nm and shoulders at +550 cm^{-1} and +2800 cm^{-1} .

Shown separately in Figure 1b are plots of the measured fragment ion yield (red) and the inferred *ePD* yield (green). *ePD* occurs over the entire wavelength range and is essentially the sole dissociation process at higher photon energies ($\lambda < 425 \text{ nm}$), whereas both *ePD* and fragmentation occur at lower photon energies ($\lambda = 445\text{--}500$

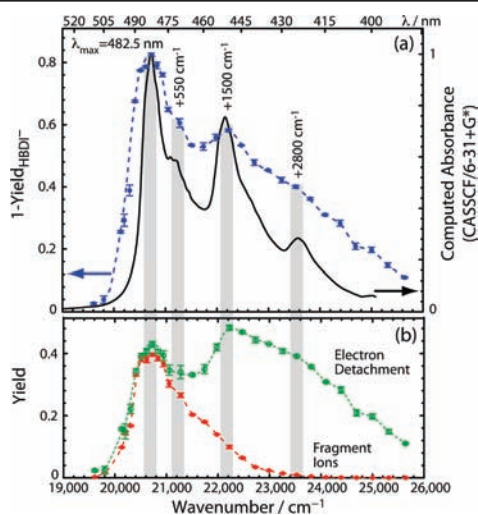


Figure 1. (a) Action spectrum of gaseous HBDI⁻ (solid blue circles) compared to the simulated absorption spectrum⁸ of HBI⁻ (black line), which has been shifted to make the computed origin (465 nm) and experimental origin (482.5 nm) coincide. (b) Individual action spectra from measured fragmentation yield (solid red circles) and inferred electron detachment (open green circles). Mass-selected HBDI⁻ was irradiated at each activation wavelength for 250 ms at a power of 4 mW.

nm). There is a striking similarity between the *fragment* ion action spectrum shown here ($\lambda_{\max} = 482.5$ nm, $\text{fwhm} \approx 30$ nm) and the ELISA data ($\lambda_{\max} = 479$ nm, $\text{fwhm} \approx 45$ nm),² implying that some or all of the products of *ePD* were not observed to an appreciable extent in the ELISA experiments. There was a dead time of ~ 15 μs in the ELISA experiments. It is probable that electron detachment (at least that activated by photon energies > 21600 cm^{-1}) occurred within the dead time. Interestingly, the dissociation kinetics, power dependence, and experiments at varying pressures and laser pulse rates indicate that electron detachment at 410 nm results from absorption of a single photon while the band at 482.5 nm results from absorption of multiple photons in the QIT.⁹

Figure 1a compares the gas-phase action spectrum of HBDI⁻ with a simulated absorption spectrum⁸ of the simplified model chromophore HBI⁻, in which the two CH₃ substituents are replaced by H atoms, as computed using CASSCF.^{5b} The unscaled simulated spectrum was convoluted with a 100 cm^{-1} line width Lorentzian⁸ and shifted to align the computed band origin with the experimental origin. Different values for the $S_0 \rightarrow S_1$ vertical excitation have been computed with CASPT2;^{5b,e} the measured transition lies between these values. The vibronic transitions computed at the CASSCF level and features measured experimentally show good agreement. The resolved peak at 450 nm (+1500 cm^{-1}) is predicted well by the calculations. Smaller features at +550 cm^{-1} (470 nm) and +2800 cm^{-1} (425 nm) are also suggested by shoulders in the experimental data. On the basis of a comparison with the simulated spectrum, the following assignments are proposed: the band at 482.5 nm is assigned to the $S_0 \rightarrow S_1$ adiabatic excitation, and the strong feature at +1500 cm^{-1} is assigned to a vertical excitation corresponding to a highly active mode of the excited state (computed at 1450 cm^{-1}) that also correlates with the computed excited-state relaxation pathway.^{5b}

At 77 K, resolved vibronic structure very similar to that observed in the room-temperature gas-phase action spectrum is apparent for

intact GFPs^{3b,c} and the model chromophore in the condensed phase.^{4f} In particular, HBDI⁻ in cold non-H-bonding solvents has a strong feature 1470 cm^{-1} away from the origin,^{4f} matching closely the 1500 cm^{-1} feature observed here.

In conclusion, no fluorescence was detected from gaseous HBDI⁻ in the ion trap; rather, electron detachment was found to be a significant mode of ion deactivation in addition to fragmentation. The extended gas-phase action spectrum (390–510 nm) exhibits vibronic activity that matches well with previous cold condensed-phase experiments and in vacuo computations. These studies illustrate the various deactivation pathways followed by the photoexcited GFP chromophore. Such knowledge of intrinsic chromophore properties is essential for understanding the photochemical mechanism behind the activity of this useful protein and its homologues.

Acknowledgment. The authors are grateful to Prof. V. M. Dong, C. Yeung, and C. Yang for the synthesis of HBDI, Prof. C. Filippi for discussions, and Prof. F. Negri for the unscaled computed spectrum. We also thank the following sources for funding: the Natural Sciences and Engineering Research Council (NSERC), the Canada Research Chairs Program, the Government of Ontario, the Estate of Margery Warren, and the Canada Foundation for Innovation (CFI).

Supporting Information Available: Experimental procedures, yield calculations, computations, supplementary figures, and additional references. This material is available free of charge via the Internet at <http://pubs.acs.org>.

References

- (a) Tsien, R. Y. *Annu. Rev. Biochem.* **1998**, *67*, 509. (b) Yang, F.; Moss, L. G.; Phillips, G. N. *Nat. Biotechnol.* **1996**, *14*, 1246. (c) Cody, C. W.; Prasher, D. C.; Westler, W. M.; Prendergast, F. G.; Ward, W. W. *Biochemistry* **1993**, *32*, 1212.
- Nielsen, S. B.; Lapierre, A.; Andersen, J. U.; Pedersen, U. V.; Tomita, S.; Andersen, L. H. *Phys. Rev. Lett.* **2001**, *87*, 228102.
- (a) Heim, R.; Prasher, D. C.; Tsien, R. Y. *Proc. Natl. Acad. Sci. U.S.A.* **1994**, *91*, 12501. (b) Chattoraj, M.; King, B. A.; Bublitz, G. U.; Boxer, S. G. *Proc. Natl. Acad. Sci. U.S.A.* **1996**, *93*, 8362. (c) Bublitz, G.; King, B. A.; Boxer, S. G. *J. Am. Chem. Soc.* **1998**, *120*, 9370. (d) Patterson, G. H.; Knobel, S. M.; Sharif, W. D.; Kain, S. R.; Piston, D. W. *Biophys. J.* **1997**, *73*, 2782.
- (a) Niwa, H.; Inouye, S.; Hirano, T.; Matsuno, T.; Kojima, S.; Kubota, M.; Ohashi, M.; Tsuji, F. I. *Proc. Natl. Acad. Sci. U.S.A.* **1996**, *93*, 13617. (b) Kojima, S.; Ohkawa, H.; Hirano, T.; Maki, S.; Niwa, H.; Ohashi, M.; Inouye, S.; Tsuji, F. I. *Tetrahedron Lett.* **1998**, *39*, 5239. (c) He, X.; Bell, A. F.; Tonge, P. J. *J. Phys. Chem. B* **2002**, *106*, 6056. (d) Litvinenko, K. L.; Webber, N. M.; Meech, S. R. *J. Phys. Chem. A* **2003**, *107*, 2616. (e) Mandal, D.; Tahara, T.; Meech, S. R. *J. Phys. Chem. B* **2004**, *108*, 1102. (f) Webber, N. M.; Meech, S. R. *Photochem. Photobiol. Sci.* **2007**, *6*, 976. (g) Dong, J.; Solntsev, K. M.; Tolbert, L. M. *J. Am. Chem. Soc.* **2006**, *128*, 12038.
- (a) Weber, W.; Helms, V.; McCammon, J. A.; Langhoff, P. W. *Proc. Natl. Acad. Sci. U.S.A.* **1999**, *96*, 6177. (b) Martin, M. E.; Negri, F.; Olivucci, M. *J. Am. Chem. Soc.* **2004**, *126*, 5452. (c) Toniolo, A.; Olsen, S.; Manohar, L.; Martinez, T. J. *Faraday Discuss.* **2004**, *127*, 149. (d) Altoe, P.; Bernardi, F.; Garavelli, M.; Orlandi, G.; Negri, F. *J. Am. Chem. Soc.* **2005**, *127*, 3952. (e) Filippi, C.; Zaccheddu, M.; Buda, F. *J. Chem. Theory Comput.* **2009**, *5*, 2074.
- (a) Forbes, M. W.; Talbot, F. O.; Jockusch, R. A. In *Practical Aspects of Trapped Ion Mass Spectrometry*; March, R. E., Todd, J. F. J., Eds.; CRC Press: Boca Raton, FL, 2009; Vol. 5, pp 239–290. (b) Bian, Q.; Forbes, M. W.; Talbot, F. O.; Jockusch, R. A. Submitted for publication.
- (a) Boesl, U.; Knott, W. *J. Mass Spectrom. Rev.* **1998**, *17*, 275. (b) Campbell, E. E. B.; Levine, R. D. *Annu. Rev. Phys. Chem.* **2000**, *51*, 65. (c) Joly, L.; Antoine, R.; Allouche, A.-R.; Broyer, M.; Lemoine, J.; Dugourd, P. *J. Am. Chem. Soc.* **2007**, *129*, 8428.
- Negri, F. Università di Bologna, Italy. Personal communication, 2009.
- Forbes, M. W.; Nagy, A. M.; Jockusch, R. A. To be submitted.

JA9066404